Available online at www.sciencedirect.com
ScienceDirect
Trans. Nonferrous Met. Soc. China 26(2016) 1878−1884
Transactions of Nonferrous Metals Society of China
www.tnmsc.cn

Microstructure and evolution of (TiB_2+Al_2O_3)/NiAl composites prepared by self-propagation high-temperature synthesis

Xiao-jie SONG[1], Hong-zhi CUI[1], Li-li CAO[1], P. Y. GULYAEV[2]

1. School of Materials Science and Engineering,
Shandong University of Science and Technology, Qingdao 266590, China;
2. Polytechnic Institute, Yugra State University, Rhanty-Mansiysk 628012, Russian Federation

Received 5 June 2015; accepted 3 March 2016

Abstract: (TiB_2+Al_2O_3)/NiAl composites were synthesized by self-propagation high-temperature synthesis, and their phase compositions, microstructures and evolution modes were studied. The microstructures and shapes vary with the TiB_2+Al_2O_3 content in the NiAl matrix. TiB_2 particles take a great variety of elementary shapes such as white bars, plates, herringbones, regular cubes and cuboids. These results outline a strategy of self-assembly processes in real time to build diversified microstructures. Some TiB_2 grains in sizes of 2−5 μm are embeded in Al_2O_3 clusters, while a small number of TiB_2 particles disperse in the NiAl matrix. It is believed that the higher the TiB_2+Al_2O_3 content is, the more the regular shapes and homogeneous distributions of TiB_2 and Al_2O_3 will be present in the NiAl matrix.

Key words: (TiB_2+Al_2O_3)/NiAl composites; self-propagation high-temperature synthesis; microstructure; evolution mechanism

1 Introduction

Due to its low density (5.59 g/cm^3), high melting point (1911 K), good thermal conductivity and good corrosion resistance [1], the NiAl intermetallic compounds have a wide application for components in high-temperature and corrosive environments, such as aero-engines, blades of gas turbine, thermal barrier coatings, and corrosion-resisting coatings. However, the low plasticity at room temperature and low strength at high temperature limit their applications in industry and production [2,3].

Up to now, many publications have involved in improving the room temperature plasticity and high temperature strength of Ni−Al intermetallic compounds. Adding different alloy elements such as Mo [4], Ti [5], Cr [6], and rare-earth metals [7] in NiAl is an efficient way to improve its properties. By adding or forming ceramics particles, such as Al_2O_3 [8,9], TiB_2 [10], NbB_2 [11] and TiC [12,13], the strength and creep properties of Ni−Al composite material can also be greatly improved. MICHALSKI et al [14] fabricated a NiAl−Al_2O_3 composite with different amounts of Al_2O_3 in NiAl through spark plasma sintering and self-propagation high-temperature synthesis (SHS) of Ni and Al, and the results showed that the hardness of NiAl−Al_2O_3 increased and the fracture toughness of it was almost twice that of NiAl. The fabrication of NiAl matrix composites was carried out by a variety of novel processes such as combustion synthesis [11,14], mechanical alloying [13] and high pressure reaction sintering. It has been proved that combustion synthesis has significant advantages, such as low energy consumption, inexpensive fabrication equipment, simplicity of operation and in situ synthesis of composite components, compared with other conventional methods. Via combustion synthesis procedure, a series of NiAl matrix composites reinforced by TiB_2, NbB_2, TiC, Al_2O_3, ZrB_2 [15] and TiN [16] were obtained conveniently.

At present, many researches focus on TiB_2 and Al_2O_3 ceramics as a duplex reinforced phase in different matrices because of their similar thermal expansion coefficient, chemical and physical compatibility [17]. By adding TiB_2 into Al_2O_3 ceramics, the growth of Al_2O_3 grains and the propagation of cracks in the matrix can be

Foundation item: Project (51272141) supported by the National Natural Science Foundation of China; Project (ts20110828) supported by the Taishan Scholars Project of Shandong Province, China; Project (2015AA034404) supported by the Ministry of Science and Technology of China
Corresponding author: Hong-zhi CUI; Tel: +86-532-86057929; E-mail: hzhcui@163.com
DOI: 10.1016/S1003-6326(16)64265-6

prevented. Consequently, the fine and well-distributed TiB_2 phase would help to enhance the strength and fracture toughness of the composite material. Thus, it would contribute to improving the abrasion resistance and fracture toughness in cutting tool materials [18,19].

The study on the previous work indicates that the fabrication of TiB_2+Al_2O_3/NiAl composite materials through combustion synthesis has not been fully investigated. The fundamental objective of the present study is to investigate the microstructures and their evolution modes when different TiB_2+Al_2O_3 contents were formed in the NiAl matrix, using Ni, Al, B_2O_3 and TiO_2 as raw materials, via combustion synthesis. Also, the correlation between the TiB_2+Al_2O_3 content, microstructure and properties of the composites was investigated.

2 Experimental

The raw materials are commercial pure Ni powder (99.9%, 38−50 μm), Al powder (99.9%, 75 μm), B_2O_3 powder (98%, 75 μm), and TiO_2 powder (98%, 45 μm). The powder mixtures were considered as two parts: one was Ni+Al in which the mole ratio was fixed to n(Ni):n(Al)=1:1, the other was Al+TiO_2+B_2O_3 in which the mole ratio was fixed to n(Al):n(TiO_2):n(B_2O_3)= 10:3:3, and the latter was added into the former in mass fractions of 0, 5%, 10%, 15%, 20%, 25% and 30%, respectively. In order to produce a homogeneous mixture, all the powders were mixed in a three− dimension blender for about 6 h. Then, the mixtures were poured into metal molds with dimensions of d20 mm × 20 mm and pressed at a pressure of 150 MPa into cylindrical compacts. Seven typical green compacts were fabricated with different contents of Al+TiO_2+B_2O_3. In order to make the reactants react completely, the green compacts were preheated in an electric furnace at 300 °C for 30 min. After that, the compacts together with the molds were taken out and a small amount of Mg powders was poured onto the surface as the initiating combustion agent. At last the compacts were ignited by live tungsten wire immediately. The reactions between powders in raw materials were as follows:

$$Ni+Al=NiAl \quad (1)$$

$$10Al+3TiO_2+3B_2O_3=3TiB_2+5Al_2O_3 \quad (2)$$

Under the present condition, the reaction in green compact could self-sustain due to its high exothermic heat (SHS), the process is shown in Fig. 1.

The crystalline phases of the products were characterized by X-ray diffraction (XRD, Model D/Max 2500PC Rigaku, Japan). The morphologies of the fracture and microstructure were observed by scanning electron microscopy (SEM, Model KYKY2800B) and field emission scanning electron microscopy (FESEM, NOVA NANOSEM 450, FEI). The compositions of samples were analyzed using electron probe microanalysis (EPMA, JXA−8230). The microhardness was measured by FM−700 with the load of 1 N and sustaining for 10 s. For each compound, five indentations were taken in the microhardness test and made an average of these points with a consideration of relative errors.

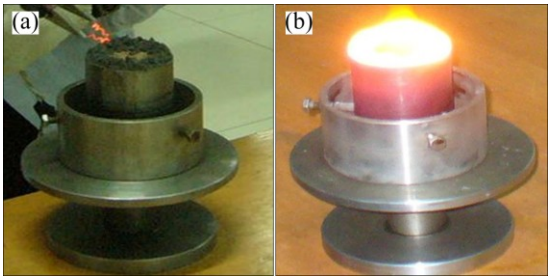

Fig. 1 Schematic diagrams of SHS reaction initiated by electrifying tungsten wire (a) and SHS reaction (b)

3 Results

In the sample without Al+TiO_2+B_2O_3, the Ni+Al reaction wave propagated steadily, and the speed was about 25 mm/s. When adding Al+TiO_2+B_2O_3 into Ni+Al, the igniting delay time prolonged. Once the reaction was initiated, the reaction wave spread rapidly. When the content of Al+TiO_2+B_2O_3 increased to 15%, the spreading speed reached up to 40 mm/s. Thus, the whole reaction in the compacts almost took place at the same time, similar to thermal explosion. After the reactions finishing, the samples were slowly cooled down.

3.1 Phase analysis

Figure 2 shows the XRD pattern of the raw materials. It illustrates that the powder mixture is composed of Ni, Al, TiO_2 and B_2O_3. Figure 3 shows the XRD patterns of products obtained by adding different contents of Al+TiO_2+B_2O_3.

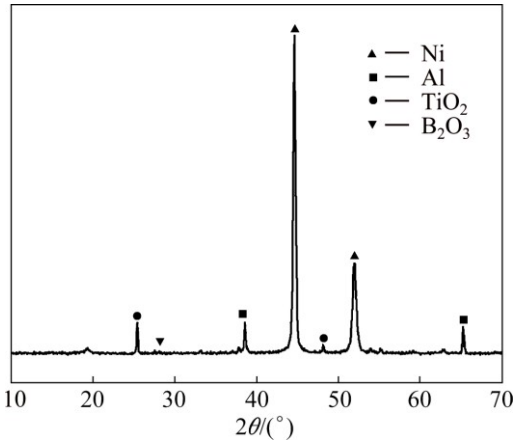

Fig. 2 XRD pattern of reactants

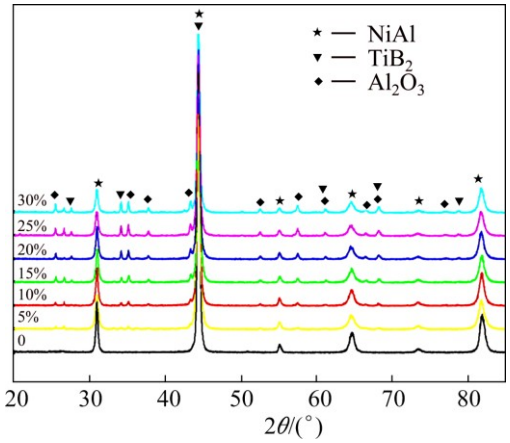

Fig. 3 XRD patterns of NiAl products with different contents of $Al+TiO_2+B_2O_3$

The reaction products simply consist of NiAl when the mixture contains only Ni and Al, which is in accordance with Reaction (1). After adding $Al+TiO_2+B_2O_3$, TiB_2 and Al_2O_3 ceramic phases appear besides NiAl phase. The higher the reactant content of $Al+TiO_2+B_2O_3$ is, the more the TiB_2 and Al_2O_3 ceramic phases can be generated. Moreover, there are hardly any unreacted raw materials. Thus, it can be deduced that the reactions were completely carried out, and the phases which are expected according to Reaction (2) are obtained.

3.2 Microstructure and hardness

The microstructures on polished surface of samples with different contents of ceramics are shown in Fig. 4. In the samples only containing Ni+Al, the NiAl grains are coarse with a lot of needles and parallel plates, as shown in Figs. 4(a) and (b), and this is in accordance with Ref. [20]. After adding $Al+TiO_2+B_2O_3$, some white bars and plates (~5 μm) distributed along the boundary of the matrix appear, and the grains of NiAl matrix are refined remarkably, as shown in Figs. 4(c) and (d). Furthermore, some plates (10−15 μm) are alternatively distributed with a kind of grey phase, and their distributional patterns are very similar to herringbone

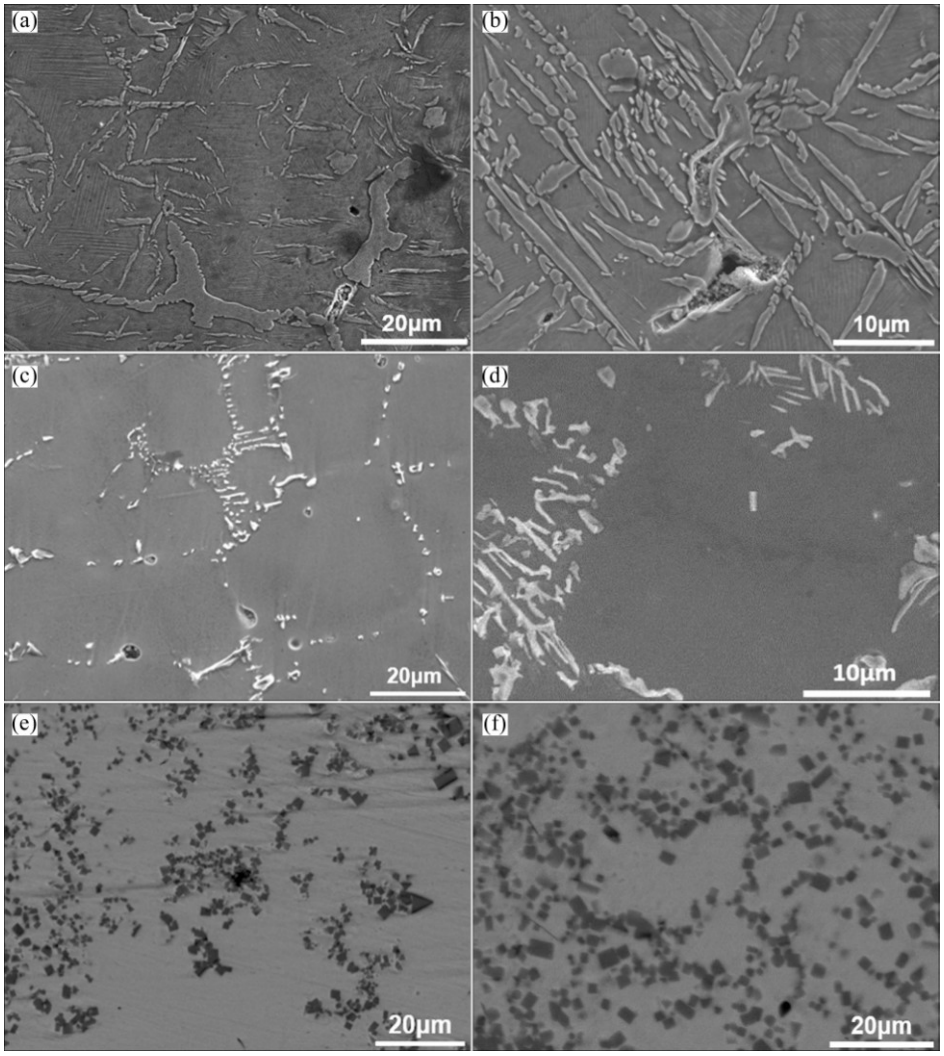

Fig. 4 SEM images of NiAl products with different contents of $Al+TiO_2+B_2O_3$: (a, b) 0; (c, d) 10%; (e) 20%; (f) 30%

structure. When the content of Al+TiO_2+B_2O_3 increases to 20% , the white phase turns to be fine regular particles (smaller than 5 μm), mainly in the shape of cubes or cuboids gathering together as clusters on an irregular dark grey conglomerations, as shown in Fig. 4(e). Also the aggregation (60−70 μm) of white particle clusters on the irregular conglomerations and some white particles still distribute along the grains boundary of the matrix. The white particles seem to be inlaid in the dark grey conglomerations. With further increasing the content of Al+TiO_2+B_2O_3, the amount of white particles increases significantly. But the size of aggregations of white particles, becomes smaller. In addition, some white particles disappear in the matrix, as shown in Fig. 4(f).

The microhardness test results are listed in Table 1. The average microhardnesses of the matrix in NiAl products without and with 10% (Al+TiO_2+B_2O_3) are HV_{100} 398 and HV_{100} 501, respectively, which are close to the hardness of pure NiAl [20]. The microhardness of herringbone structure in the product with 10% (Al+TiO_2+B_2O_3) is HV_{100} (1160−1730), which fluctuates remarkably. Compared with the product with 10% (Al+TiO_2+B_2O_3), the hardness of white cube or cuboids gathering clusters in the products with 20% and 30% (Al+TiO_2+B_2O_3) is higher, and the highest hardness is up to HV_{100} 2700. The hardness of dark grey irregular conglomerations which look like being pinned under the cube or cuboid particles is HV_{100} (1260−1480). The hardness of the products with 20% and 30% (Al+TiO_2+B_2O_3) also varies from HV_{100} 570 to HV_{100} 1420, and the highest hardness is close to that of dark grey conglomerations.

Table 1 Microhardness and adiabatic temperature of samples with different contents of Al+TiO_2+B_2O_3

Sample	Microhardness (HV)	Adiabatic temperature/K
Pure NiAl	398±19	1911
NiAl−5%(TiB_2−Al_2O_3)	410±21	1938
NiAl−10%(TiB_2−Al_2O_3)	501±25	1965
NiAl−15%(TiB_2−Al_2O_3)	567±28	1992
NiAl−20%(TiB_2−Al_2O_3)	595±29	2018
NiAl−25%(TiB_2−Al_2O_3)	608±31	2045
NiAl−30%(TiB_2−Al_2O_3)	596±30	2072
Pure (TiB_2−Al_2O_3)	−	2448

3.3 Composition

The SEM images of typical samples and the results of EDS composition analysis are shown in Fig. 5 and Tables 2 and 3, respectively. Combining the results of XRD analysis, microhardness test and EDS composition analysis, we can deduce that the white bars and plates which distribute along the boundary of the matrix or in herringbone structure at Spectrum 1 in Fig. 5(a) and the white particles in regular cube or cuboids shapes shown in Figs. 4(e) and (f) and Spectrum 3 in Fig. 5(b) are all TiB_2 grains. The gray matrix shown in Figs. 4(a) and (c) and Spectrum 2 in Figs. 5(a) and (b) is NiAl intermetallic compound. The irregular dark grey clusters which are around or under the cube or cuboids particles in Figs. 4(e) and (f) and Spectrum 3 in Figs. 5(a) and (b) are Al_2O_3.

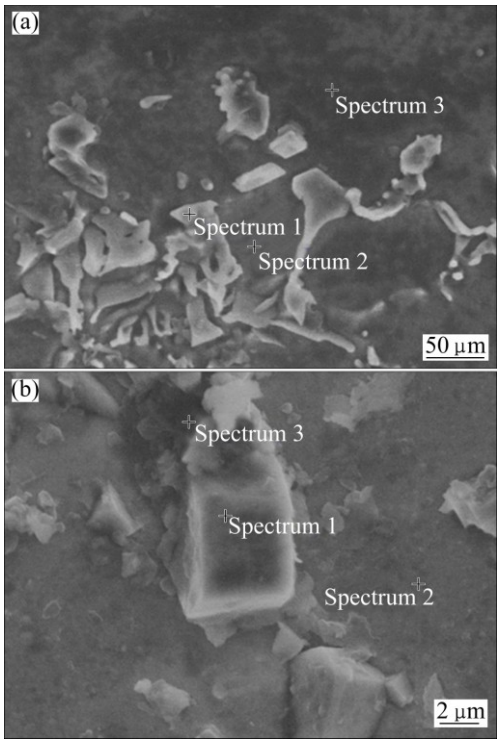

Fig. 5 SEM images of products with different contents of Al+TiO_2+B_2O_3: (a) 5%; (b) 15%

Table 2 EDS compositions of composite with 5% (Al+TiO_2+B_2O_3)

Element	*x*/%		
	Spectrum 1	Spectrum 2	Spectrum 3
Ni	0	46.27	6.47
Al	0	50.34	39.17
Ti	33.43	0	0
B	66.56	0	0
O	0	3.39	54.36

Table 3 EDS compositions of composite with 15% (Al+TiO_2+B_2O_3)

Element	*x*/%		
	Spectrum 1	Spectrum 2	Spectrum 3
Ni	0	41.33	5.23
Al	0	52.36	37.27
Ti	30.75	0	0
B	69.24	0	0
O	0	6.31	57.50

4 Discussion

The mixture of reactants could be considered as two parts: one is Ni+Al which follows Reaction (1), the other is Al+TiO_2+B_2O_3 which follows Reaction (2). If the reaction systems are initiated at room temperature, the adiabatic temperature of Reaction (1) would be T_{ad}=$T_{m,NiAl}$=1911 K [21], while the adiabatic temperature of Reaction (2) would be T_{ad}=2448 K [22]. When preheating the samples at 300 °C, the adiabatic temperatures of Reactions (1) and (2) at 300 °C are much higher than their T_{ad} at room temperature. The T_{ad} of Ni+Al+TiO_2+B_2O_3 hybrid system can be calculated according to the thermodynamic data provided in Ref. [23]. With the increase of Al+TiO_2+B_2O_3 content, the T_{ad} of the mixtures rises to above 1911 K. The adiabatic temperatures of samples with different mass fractions of Al+TiO_2+B_2O_3 are listed in Table 1.

The reaction processes and microstructure evolution mechanisms of the system are shown in Fig. 6. As the melting points of Al and B_2O_3 are 660 and 445 °C, respectively, Al and B_2O_3 in the green powder (Fig. 6(a)) melt firstly during the reaction proces. The melted Al contacts with liquid B_2O_3 and infiltrates into the surface of TiO_2 particles, as shown in Fig. 6(b). Thus, B and Ti elements are displaced from B_2O_3 and TiO_2, respectively [24,25]. At the same time, Al_2O_3 and TiB_2 are produced rapidly through Reaction (2). Moreover, the surplus molten Al and solid Ni react to from liquid NiAl, as the melting point of NiAl is lower than the adiabatic temperature of reaction system, as shown in Fig. 6(c). The sequences of the whole reaction are as follows:

$$Ni+Al \longrightarrow NiAl \quad (3)$$

$$2Al+B_2O_3 \longrightarrow Al_2O_3+2B \quad (4)$$

$$4Al+3TiO_2 \longrightarrow 2Al_2O_3+3Ti \quad (5)$$

$$Ti+2B \longrightarrow TiB_2 \quad (6)$$

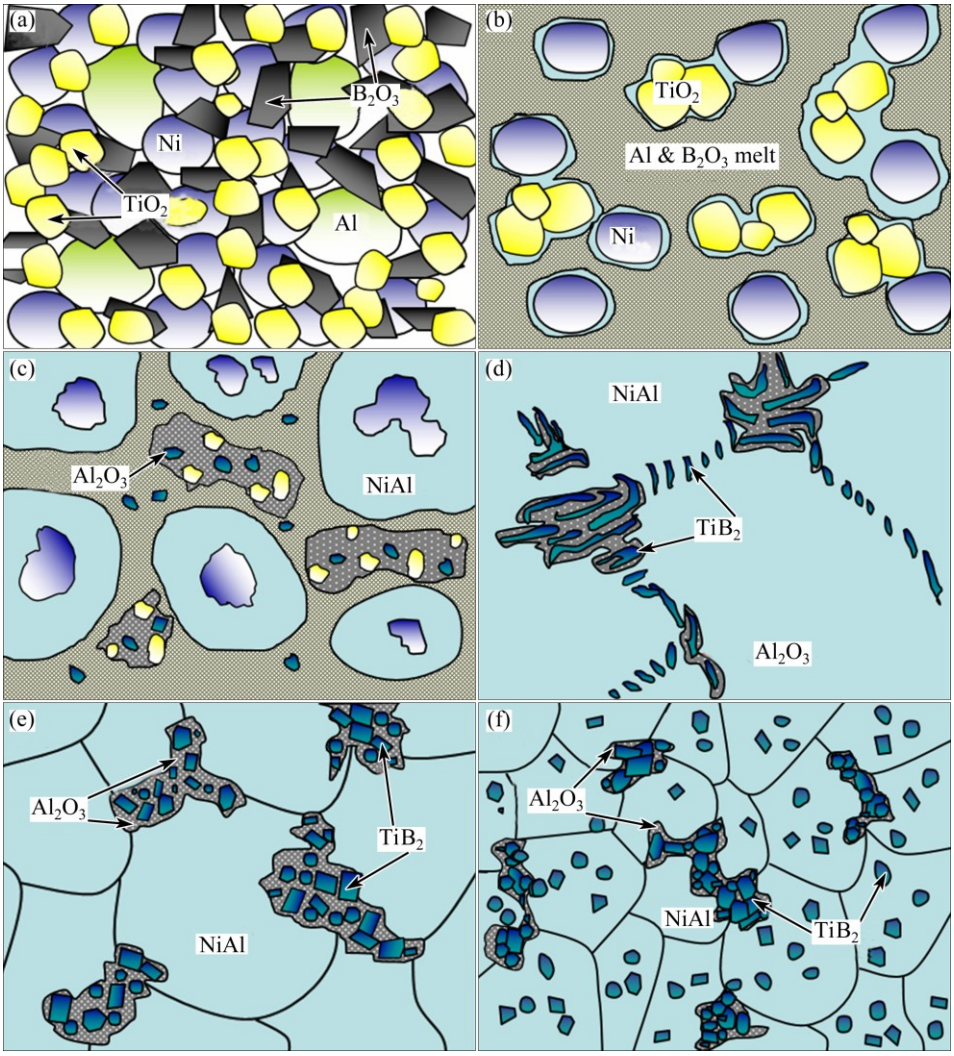

Fig. 6 Sketch of reaction processes and structure evolution modes: (a) Mixed initial powders; (b) Al and B_2O_3 begin to melt; (c) Grains of NiAl, TiB_2 and Al_2O_3 formatting; (d−f) Morphologies of products with 10%, 20% and 30% (Al+TiO_2+B_2O_3), respectively

When the content of Al+TiO_2+B_2O_3 is less than 10%, both the amounts of TiB_2 and Al_2O_3, and the temperature of the reaction system are not sufficient. Therefore, the TiB_2 grains grow as irregular bars and plates [26,27] (Figs. 4(d) and 6(d)). TiB_2 and Al_2O_3 grow into herringbone alternative structure through "self-assembly" mode. When the reaction system cools down below the NiAl meting point, NiAl grains begin to nuclear and grow to form the matrix of composite gradually.

With increasing the content of Al+TiO_2+B_2O_3, the T_{ad} of reaction system increases and a great amount of TiB_2 and Al_2O_3 is produced. The abundant TiB_2 resources and higher temperature are better for the regularization of TiB_2 [26]. Thus, TiB_2 particles grow freely, develop fully and take shapes of cube or cuboids finally. As Al_2O_3 grains form around the TiB_2 grains almost simultaneously, it is possible for them to attach together to form large irregular conglomerations, as shown in Figs. 4(e) and (f) and 6(e) and (f). During the grow process of NiAl grains, the conglomerations are pushed to the corner of grains or distribute along the boundaries. Also, this kind of distribution impedes the boundary's movement and restricts the grain's growth of NiAl matrix.

When the Al+TiO_2+B_2O_3 content increases to 30%, much higher T_{ad} can be reached and more TiB_2 and Al_2O_3 are produced. All the above contribute a lot to TiB_2 grains to grow as regular cubes cuboids or hexagons, as shown in Figs. 4(e) and (f) and 7(a). In addition, a large amount of Al_2O_3 adheres to TiB_2 grains to nuclear, as shown in Fig. 7(b), and grows around them. Because there are no plates to subdivide the spaces between TiB_2 grains, as shown in Fig. 4(b), the Al_2O_3 grains develop more freely until touching each other to form conglomerations, as shown in Figs. 4(c) and (d). In the meantime, there are also some single TiB_2 cubes or cuboids dispersed in the NiAl liquid and some Al_2O_3 grains adhere to the impurities in NiAl liquid to nuclear. Finally, when NiAl begins to solidify, almost all the above solid phases that form before NiAl will be pushed to the grain boundaries in the similar way shown in Figs. 4(b) and 6(e), which makes contribution to the formation of refine NiAl grains. What is more, the Al_2O_3 grains which nucleate on the impurities may remain in the NiAl matrix to help to improve the hardness. These Al_2O_3 grains may flock together and become big conglomerations because of the self-diffusion of Al_2O_3. Therefore, the hardness of matrix in Fig. 4(c) varies greatly, and the highest hardness is close to that of pure conglomerations.

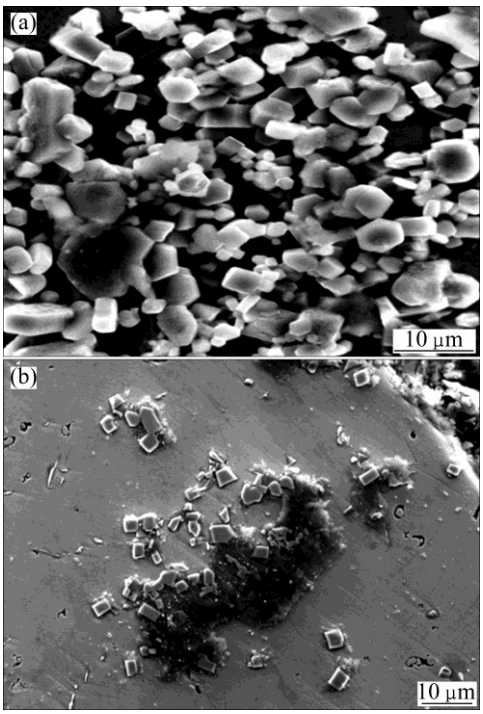

Fig. 7 SEM images of regular TiB_2 particles (a) and Al_2O_3 conglomerations (b)

5 Conclusions

1) (TiB_2+Al_2O_3)/NiAl composites were synthesized by combustion synthesis using Ni, Al, TiO_2 and B_2O_3 mixed powders. With increasing the content of Al+TiO_2+B_2O_3, more TiB_2 and Al_2O_3 ceramic phases are generated in the NiAl matrix. When the reactant content of Al+TiO_2+B_2O_3 is less than 10%, TiB_2 and Al_2O_3 grow into herringbone alternative structure through self-assembly mode.

2) When more TiB_2+Al_2O_3 form, TiB_2 particles would grow freely and develop fully and take shapes of cube, cuboids or hexagons finally. At the same time, more Al_2O_3 which forms around TiB_2 grains tends to attach together to form large irregular conglomerations.

3) The microhardness of NiAl matrix composite increases by 50% from HV (398±19) to HV (608±31), due to grain refining with increasing the content of TiB_2+Al_2O_3 to 25%.

References

[1] OZDEMIR O, ZEYTIN S, BINDAL S. A study on NiAl produced by pressure-assisted combustion synthesis [J]. Vacuum, 2010, 84: 430−437.

[2] FANG H C, XIAO P, XIONG X, YU G J. Microstructures, mechanical and oxidation behaviors of C/C composites modified by NiAl alloy [J]. Transactions of Nonferrous Metals Society of China, 2016, 26(1): 196−202.

[3] ADABI M, AMADEH A A. Formation mechanisms of Ni−Al intermetallics during heat treatment of Ni coating on 6061 Al substrate [J]. Transactions of Nonferrous Metals Society of China, 2015, 25(12): 3959−3966.

[4] RAY P K, AKINC M, KRAMER M J. Formation of multilayered scale during the oxidation of NiAl−Mo alloy [J]. Applied Surface

Science, 2014, 301: 107−111.
[5] RIYADI T W B, ZHANG T, MARCHANT D, ZHU X M. Synthesis and fabrication of NiAl coatings with Ti under layer using induction heating [J]. Surface and Coatings Technology, 2014, 258(6): 154−159.
[6] TANAK Y, OIKAW K, SUTOU Y, OMORI T, KAINUMA R, ISHIDA K. Martensitic transition and super elasticity of Co−Ni−Al ferromagnetic shape memory alloys with two-phase structure [J]. Materials Science and Engineering A, 2006, 438: 1054−1060.
[7] GUO J T, YUAN C, HOU J S. Effects of rare earth elements on NiAl-based alloys [J]. Acta Metallurgica Sinica, 2008, 44(5): 513−520. (in Chinese)
[8] SHENG L Y, YANG F, XI T F, GUO J T, YE H Q. Microstructure evolution and mechanical properties of Ni_3Al/Al_2O_3 composite during self-propagation high-temperature synthesis and hot extrusion [J]. Materials Science and Engineering A, 2012, 555(41): 131−138.
[9] YANG W, DONG S J, LUO P, YANGLI A Z, LIU Q, XIE Z X. Effect of Ni addition on the preparation of Al_2O_3–TiB_2 composites using high-energy ball milling [J]. Journal of Asian Ceramic Societies, 2004, 2(4): 399−402.
[10] CUI H Z, MA L, CAO L L, TENG F L, CUI N. Effect of NiAl content on phases and microstructures of TiC−TiB_2−NiAl composites fabricated by reaction synthesis [J]. Transactions of Nonferrous Metals Society of China, 2014, 24(2): 346−353.
[11] SHOKATI A A, PARVIN N, SABZIANPOUR N, SHOKATI M, HEMMATI A. In situ synthesis of NiAl−NbB_2 composite powder through combustion synthesis [J]. Journal of Alloys and Compounds, 2013, 549(5): 141−146.
[12] SHENG L Y, YANG F, GUO J T, XI T F, YE H Q. Investigation on NiAl−TiC−Al_2O_3 composite prepared by self-propagation high temperature synthesis with hot extrusion[J]. Composites Part B: Engineering, 2013, 45(1): 785−791.
[13] MOHAMMAD M, SHAMANIAN M, ENAYATI M H, SALEHI M, HOSEYNIAN A. Microstructures and properties of NiAl−TiC nanocomposite coatings on carbon steel surfaces produced by mechanical alloying technique [J]. Surface and Coatings Technology, 2014, 238: 180−187.
[14] MICHALSKI A, JAROSZEWICZ J, ROSIŃSKI M, SIEMIASZKO D. NiAl−Al_2O_3 composites produced by pulse plasma sintering with the participation of the SHS reaction [J]. Intermetallics, 2006, 14(6): 603−606.
[15] CAMURLU H E, MAGLIA F. Self-propagating high-temperature synthesis of ZrB_2 or TiB_2 reinforced Ni−Al composite powder [J]. Journal of Alloys and Compounds, 2009, 478(1): 721−725.
[16] SHOKATI A A, PARVIN N, SHOKATI M. Combustion synthesis of NiAl matrix composite powder reinforced by TiB_2 and TiN particulates from Ni−Al−Ti−BN reaction system[J]. Journal of Alloys and Compounds, 2014, 585(3): 637−643.
[17] LIU J, OWNBY P D. Enhanced mechanical properties of alumina by dispersed titanium diboride particulate inclusions [J]. Journal of the American Ceramic Society, 1991, 74(1): 241−243.
[18] GU M L, HUANG C Z, XIAO S R, LIU H L. Improvements in mechanical properties of TiB_2 ceramics tool materials by the dispersion of Al_2O_3 particles [J]. Materials Science and Engineering A, 2008, 486(1−2): 167−170.
[19] DENG J X, CAO T K, LIU L L. Self-lubricating behaviors of Al_2O_3/TiB_2 ceramic tools in dry high-speed machining of hardened steel [J]. Journal of the American Ceramic Society, 2005, 25(7): 1073−1079.
[20] CUI H Z, WEI N, ZENG L L, WANG X B, TANG H J. Microstructure and formation mechanism of Ni−Al intermetallic compounds fabricated by reaction synthesis [J]. Transactions of Nonferrous Metals Society of China, 2013, 23(6): 1639−1645.
[21] ZHU P, LI J C M, LIU C T Adiabatic temperature of combustion synthesis of Al−Ni systems [J]. Materials Science and Engineering A, 2003, 357(357): 248−257.
[22] MEYERS M A, OLEVSKY E A, MA J, JAMET M. Combustion synthesis/densification of an Al_2O_3−TiB_2 composite [J]. Materials Science and Engineering A, 2001, 311(1−2): 83−99.
[23] MA Z, JI X W, LIN P, DONG S Z, LI Z C. Thermo dynamics and kinetics analysis of composite ceramic coatings Al−TiO_2−B_2O_3 system [J]. Bulletin of the Chinese Ceramic Society, 2010, 29(3): 582−587. (in Chinese)
[24] ZHU H G, WANG H Z, GE L Q, CHEN S, WU S Q. Formation of composites fabricated by exothermic dispersion reaction in A1−TiO_2−B_2O_3 system [J]. Transactions of Nonferrous Metals Society of China, 2007, 17(3): 590−594.
[25] SHARIFI E M, KARIMZADEH F, ENAYATI M H. Synthesis of titanium diboride reinforced alumina matrix nanocomposite by mechanochemical reaction of Al−TiO_2−B_2O_3 [J]. Journal of Alloys and Compounds, 2010, 502(2): 508−512.
[26] LI P T, WU Y Y, LIU X F. Controlled synthesis of different morphologies of TiB_2 microcrystals by aluminum melt reaction method [J]. Materials Research Bulletin, 2013, 48(6): 2044−2048.
[27] CHENG E J, KATSUI H, TU R, GOTO T. Rod-like eutectic structure of arc-melted TiB_2–TiC_xN_{1-x} composite [J]. Journal of the European Ceramic Society, 2014, 34(9): 2089−2094.

自蔓延高温合成(TiB_2+Al_2O_3)/NiAl复合材料的显微组织及演化机制

宋晓杰[1]，崔洪芝[1]，曹丽丽[1]，P. Y. GULYAEV[2]

1. 山东科技大学 材料科学与工程学院，青岛 266590；
2. Polytechnic Institute, Yugra State University, Rhanty-Mansiysk 628012, Russian Federation

摘 要：采用自蔓延高温合成技术制备(TiB_2+Al_2O_3)增强NiAl基复合材料，并研究其相组成、显微组织和演化机制。结果表明：复合材料的组织及陶瓷相的形貌随添加(TiB_2+Al_2O_3)含量的不同而变化，TiB_2在短时间内以自组装的模式形成长条状、片状、鱼骨状以及规则的四方体和六棱柱等不同形态。TiB_2的尺寸在2~5 μm之间，与不规则的Al_2O_3伴生存在，少量TiB_2分布于NiAl基体中。随着陶瓷相含量的增多，TiB_2的形状趋于规则，且在NiAl基体中的分布更加均匀。

关键词：(TiB_2+Al_2O_3)/NiAl复合材料；自蔓延高温合成；显微组织；演化机制

(Edited by Mu-lan QIN)